

UNIVERSITY OF OSLO



Spacetime Ripples from Domain-Wall Wiggles

On the analytical prediction of the
gravitational-wave signature from perturbed
topological defects in expanding spacetime

Nanna Bryne

Institute of Theoretical Astrophysics

Master's presentation

12th December 2024



Contents

- 1 Background
- 2 Project
- 3 Analysis
- 4 Foreground

Background

Contents

1 Background

- Thesis
- Gravitational physics
- Cosmology
- Phase transitions

2 Project

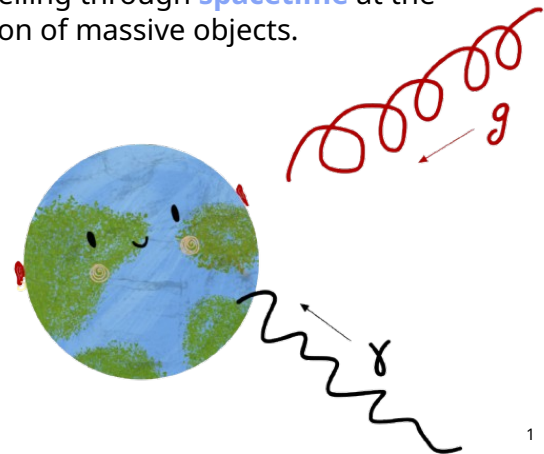
3 Analysis

4 Foreground

Spacetime ripples from domain-wall wiggles

Spacetime ripples from domain-wall wiggles

Gravitational waves (GWs) are **ripples** travelling through **spacetime** at the speed of light, generated by the acceleration of massive objects.



Spacetime ripples from domain-wall wiggles

Gravitational waves (GWs) are **ripples** travelling through **spacetime** at the speed of light, generated by the acceleration of massive objects.

Potential sources of low-frequency GWs are topological defects, such as spatially perturbed—«**wiggly**»—**domain walls** (DWs).

Spacetime ripples from domain-wall wiggles

Gravitational waves (GWs) are **ripples** travelling through **spacetime** at the speed of light, generated by the acceleration of massive objects.

Potential sources of low-frequency GWs are topological defects, such as spatially perturbed—«**wiggly**»—**domain walls** (DWs).

MAIN AIM. Gain *analytical* insight to the dynamics of cosmic DWs in conformally flat Friedmann–Lemaître–Robertson–Walker (FLRW) spacetime, to search for its GW footprint.

Spacetime ripples from domain-wall wiggles

Gravitational waves (GWs) are **ripples** travelling through **spacetime** at the speed of light, generated by the acceleration of massive objects.

Potential sources of low-frequency GWs are topological defects, such as spatially perturbed—«**wiggly**»—**domain walls** (DWs).

MAIN AIM. Gain *analytical* insight to the dynamics of cosmic DWs in conformally flat Friedmann–Lemaître–Robertson–Walker (FLRW) spacetime, to search for its GW footprint.

But why?

Motivation

RELEVANCE Recent observations* provide evidence for a stochastic GW background (GWB) in cosmological frequency ranges. Future GW experiments aim at similar frequency ranges.

* Agazie et al. ((2023))

Motivation

RELEVANCE Recent observations provide evidence for a stochastic GW background (GWB) in cosmological frequency ranges. Future GW experiments aim at similar frequency ranges.

DEMAND Analytical estimates allow possibly arbitrary dynamical ranges; ranges inaccessible in cosmological simulations.

Motivation

RELEVANCE Recent observations provide evidence for a stochastic GW background (GWB) in cosmological frequency ranges. Future GW experiments aim at similar frequency ranges.

DEMAND Analytical estimates allow possibly arbitrary dynamical ranges; ranges inaccessible in cosmological simulations.

CONVENIENCE Substitution to computationally expensive relativistic simulations.

Motivation

RELEVANCE Recent observations provide evidence for a stochastic GW background (GWB) in cosmological frequency ranges. Future GW experiments aim at similar frequency ranges.

DEMAND Analytical estimates allow possibly arbitrary dynamical ranges; ranges inaccessible in cosmological simulations.

CONVENIENCE Substitution to computationally expensive relativistic simulations.

APPLICABILITY Topological defects are ubiquitous in physics.

Motivation

RELEVANCE Recent observations provide evidence for a stochastic GW background (GWB) in cosmological frequency ranges. Future GW experiments aim at similar frequency ranges.

DEMAND Analytical estimates allow possibly arbitrary dynamical ranges; ranges inaccessible in cosmological simulations.

CONVENIENCE Substitution to computationally expensive relativistic simulations.

APPLICABILITY Topological defects are ubiquitous in physics.

SIMPLICITY DWs are good pedagogies for topological defects.

Motivation

RELEVANCE Recent observations provide evidence for a stochastic GW background (GWB) in cosmological frequency ranges. Future GW experiments aim at similar frequency ranges.

DEMAND Analytical estimates allow possibly arbitrary dynamical ranges; ranges inaccessible in cosmological simulations.

CONVENIENCE Substitution to computationally expensive relativistic simulations.

APPLICABILITY Topological defects are ubiquitous in physics.

SIMPLICITY DWs are good pedagogies for topological defects.

Gravitational physics

Newtonian mechanics describe gravitation as an attractive force between massive objects.

Gravitational physics

Newtonian mechanics describe gravitation as an attractive force between massive objects.

In **general relativity** (GR), gravitation is interpreted as an intrinsic property of spacetime curvature.

Gravitational physics

In **general relativity** (GR), gravitation is interpreted as an intrinsic property of spacetime curvature. The existence of GWs is a consequence of GR.

General relativity

Curvature of spacetime manifold \mathcal{M} is described by

$$\overbrace{ds^2}^{\text{line element}} = \overbrace{g_{\mu\nu}}^{\text{metric}} dx^\mu dx^\nu. \quad (1)$$

The components obey the Einstein equations:

$$\mathcal{G}_{\mu\nu} = 8\pi G_N T_{\mu\nu}. \quad (2)$$

Here, $\mathcal{G}_{\mu\nu} = \mathcal{R}_{\mu\nu} - g_{\mu\nu}\mathcal{R}/2$ is the Einstein tensor, $\mathcal{R}_{\mu\nu}$ (\mathcal{R}) the Ricci tensor (scalar), and $T_{\mu\nu}$ the stress-energy (SE) tensor.

General relativity

Curvature of spacetime manifold \mathcal{M} is described by

$$\overbrace{ds^2}^{\text{line element}} = \overbrace{g_{\mu\nu}}^{\text{metric}} dx^\mu dx^\nu. \quad (1)$$

The components obey the Einstein equations:

$$\mathcal{G}_{\mu\nu} = 8\pi G_N T_{\mu\nu}. \quad (2)$$

SPECIAL RELATIVITY. $g_{\mu\nu} = \eta_{\mu\nu} = \text{diag}(-1, +1, +1, +1) = \text{Minkowski metric}$

FLAT, EXPANDING UNIVERSE. $g_{\mu\nu} = a^2(x^0)\eta_{\mu\nu} = (\text{flat}) \text{FLRW metric}$

Quick look: Metric perturbations

Under $g_{\mu\nu} \rightarrow \mathring{g}_{\mu\nu} = g_{\mu\nu} + \delta g_{\mu\nu}$, we get the linearised Einstein equations

$$\mathring{\mathcal{G}}_{\mu\nu} = 8\pi G_N \mathring{T}_{\mu\nu}. \quad (3)$$

MINKOWSKI. $\mathring{g}_{\mu\nu} = \eta_{\mu\nu} + h_{\mu\nu}$

FLAT FLRW. $\mathring{g}_{\mu\nu} = a^2(x^0) [\eta_{\mu\nu} + h_{\mu\nu}]$

Quick look: Metric perturbations

Under $g_{\mu\nu} \rightarrow \mathring{g}_{\mu\nu} = g_{\mu\nu} + \delta g_{\mu\nu}$, we get the linearised Einstein equations

$$\mathring{\mathcal{G}}_{\mu\nu} = 8\pi G_N \mathring{T}_{\mu\nu}. \quad (3)$$

MINKOWSKI. $\mathring{g}_{\mu\nu} = \eta_{\mu\nu} + h_{\mu\nu} \quad \cdots \Rightarrow \square_M h_{ij} \propto T_{ij}$

FLAT FLRW. $\mathring{g}_{\mu\nu} = a^2(x^0) [\eta_{\mu\nu} + h_{\mu\nu}] \quad \cdots \Rightarrow \square h_{ij} \propto a^{-2} T_{ij}$

Background cosmology

COSMOLOGICAL PRINCIPLE. *The universe is homogeneous and isotropic.*

Background cosmology

COSMOLOGICAL PRINCIPLE. *The universe is homogeneous and isotropic.*

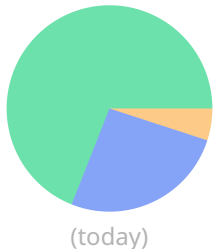
Model universe from perfect fluids s with equation of state (e.o.s.) $p_s = w_s \rho_s$. Hubble parameter is

$$H^2(a) = H_0^2 \sum_s \Omega_{s0} a^{-3(1+w_s)}. \quad (4)$$

Background cosmology

COSMOLOGICAL PRINCIPLE. *The universe is homogeneous and isotropic.*

Model universe from perfect fluids s with equation of state (e.o.s.) $p_s = w_s \rho_s$. Hubble parameter is



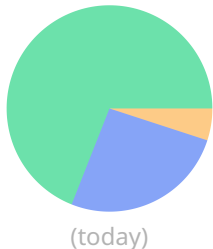
$$H^2(a) = H_0^2 \sum_s \Omega_{s0} a^{-3(1+w_s)} = H_0^2 (\Omega_{m0} a^{-3} + \Omega_{de0}). \quad (4)$$

Λ CDM. Dark energy (DE) \leftrightarrow a cosmological constant (Λ) + baryonic & cold dark matter (CDM).

Background cosmology

COSMOLOGICAL PRINCIPLE. *The universe is homogeneous and isotropic.*

Model universe from perfect fluids s with equation of state (e.o.s.) $p_s = w_s \rho_s$. Hubble parameter is



$$H^2(a) = H_0^2 \sum_s \Omega_{s0} a^{-3(1+w_s)} = H_0^2 \left(\Omega_{m0} a^{-3} + \Omega_{de0} \right). \quad (4)$$

Λ CDM. Dark energy (DE) \leftrightarrow a cosmological constant (Λ) + baryonic & cold dark matter (CDM).

- **HUBBLE TENSION.** There is a discrepancy between measurements of the Hubble constant $H_0 = 100h \text{ km s}^{-1} \text{ Mpc}^{-1}$:

“Late universe” measurements $\sim h \sim 0.73 \pm 0.02$

“Early universe” measurements $\sim h \sim 0.67 \pm 0.01$

- **HUBBLE TENSION.** There is a discrepancy between measurements of the Hubble constant $H_0 = 100h \text{ km s}^{-1} \text{ Mpc}^{-1}$:

“Late universe” measurements $\sim h \sim 0.73 \pm 0.02$

“Early universe” measurements $\sim h \sim 0.67 \pm 0.01$

- **POSSIBLE SOLUTION.** A common work-around is to let DE have time-dependent e.o.s. parameter $w_{\text{de}} = w_{\text{de}}(a)$, which can be ensured by a dynamical scalar field ϕ (cf. (a) **symmetron** , * quintessence, phantom dark energy).

*Hinterbichler et al. ((2011)); Perivolaropoulos & Skara ((2022))

The [symmetron](#) effective potential is

$$V_{\text{eff}}(\phi) = \frac{\lambda}{4}\phi^4 + \frac{\mu^2}{2}(v - 1)\phi^2, \quad (5)$$

where $v \equiv \rho_{(m)} / \rho_* \simeq (a_*/a)^3$.

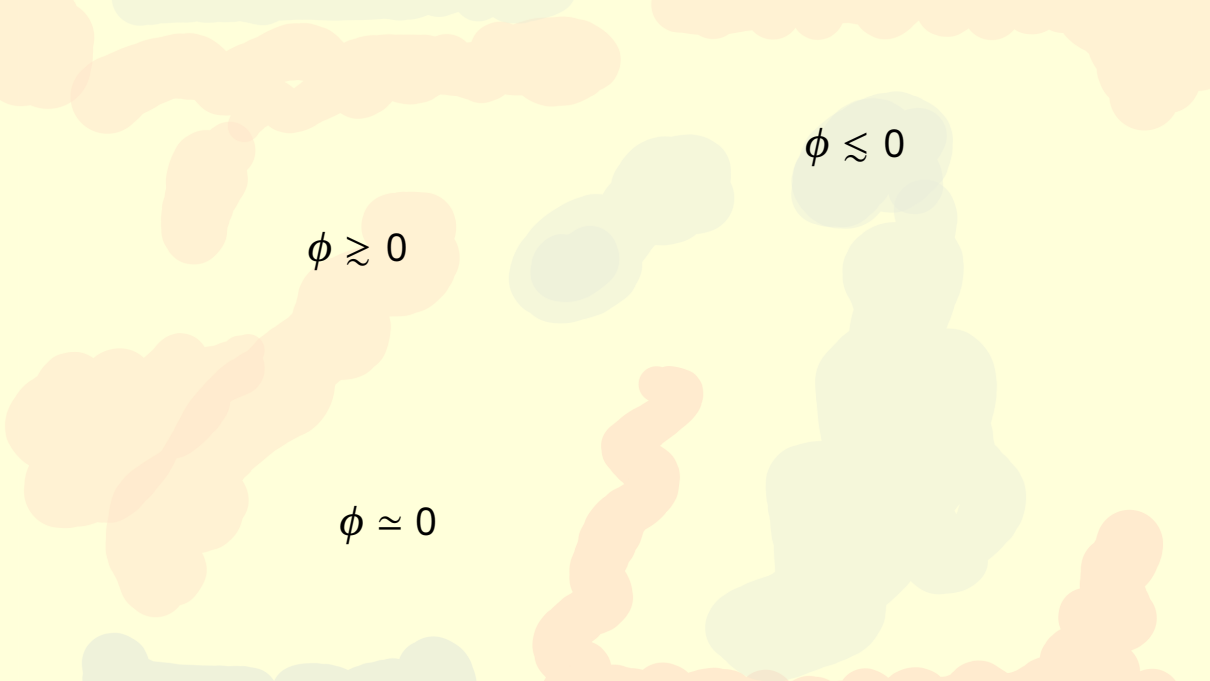
Symmetry breaking at critical density ρ_* .

The **asymmetron** effective potential is

$$V_{\text{eff}}(\phi) = \frac{\lambda}{4}\phi^4 - \frac{\kappa}{3}\phi^3 + \frac{\mu^2}{2}(v-1)\phi^2, \quad (5)$$

where $v \equiv \rho_{(m)} / \rho_* \simeq (a_*/a)^3$.

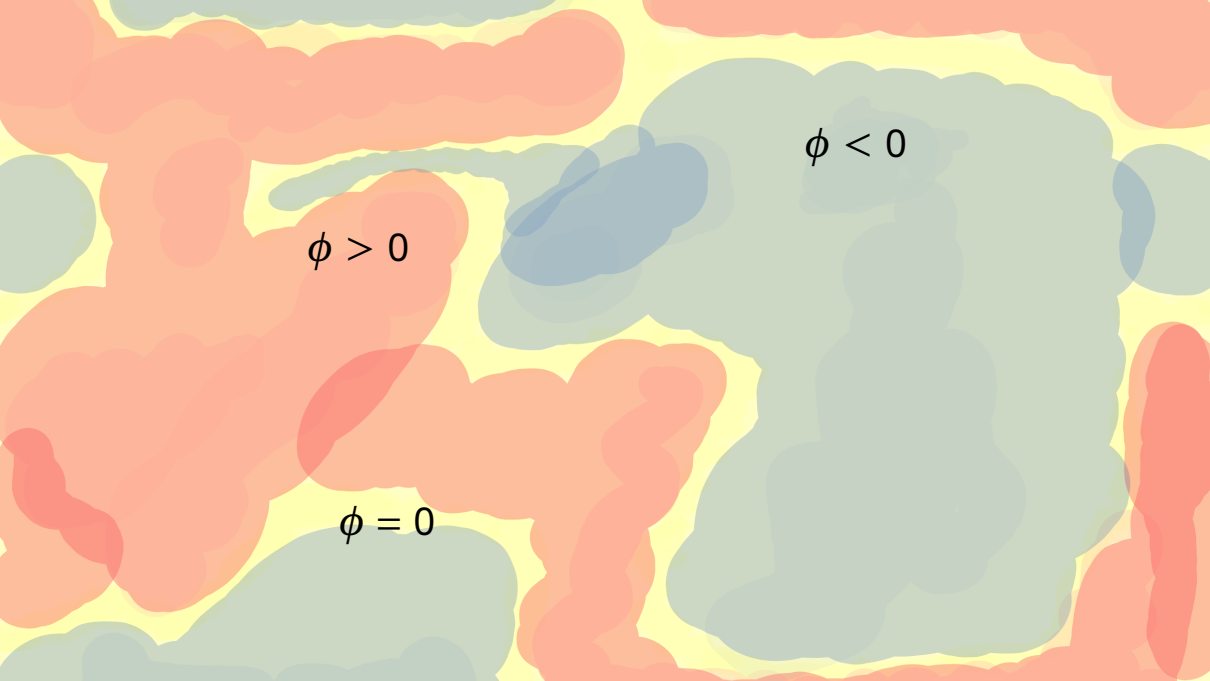
Symmetry breaking at critical density ρ_* .



$\phi \lesssim 0$

$\phi \gtrsim 0$

$\phi \simeq 0$



$\phi < 0$

$\phi > 0$

$\phi = 0$

$$\phi = \phi_-$$
$$\phi = \phi_+$$
$$\phi = 0$$

The domain-wall ripple effect

GWs from DWs are expected to be within reach of future experiments.

The domain-wall ripple effect

GWs from DWs are expected to be within reach of future experiments.

***OVERCLOSING PROBLEM.** A DW network modelled as a perfect fluid will have e.o.s.-parameter $w_{\text{dw}} = -2/3$. As contributor to the total energy budget of the universe, it would quickly dominate.

The domain-wall ripple effect

GWs from DWs are expected to be within reach of future experiments.

***OVERTCLOSING PROBLEM.** A DW network modelled as a perfect fluid will have e.o.s.-parameter $w_{\text{dw}} = -2/3$. As contributor to the total energy budget of the universe, it would quickly dominate.

***PROPOSED SOLUTIONS.** Slightly broken vacuum degeneracy; $V(\phi_+) \neq V(\phi_-)$ (e.g. asymmetron), or let walls melt away.

Project

Contents

1 Background

2 Project

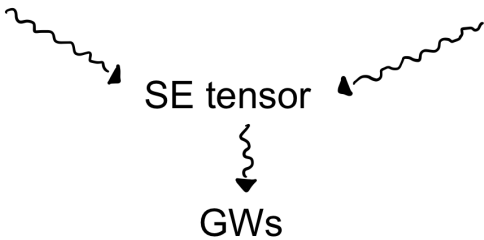
- Overview
- DW \leftrightarrow hypersurface
- DW \leftrightarrow scalar field

3 Analysis

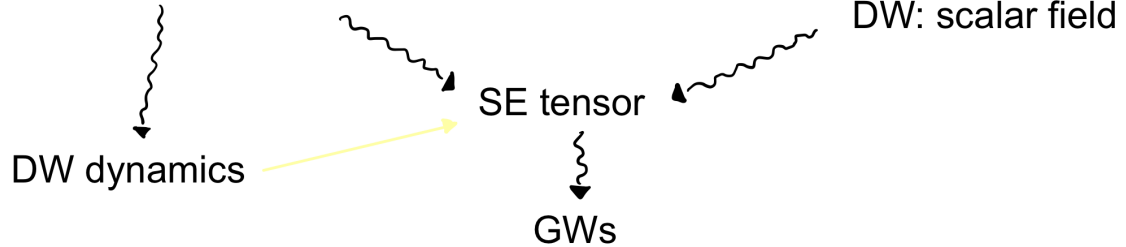
4 Foreground

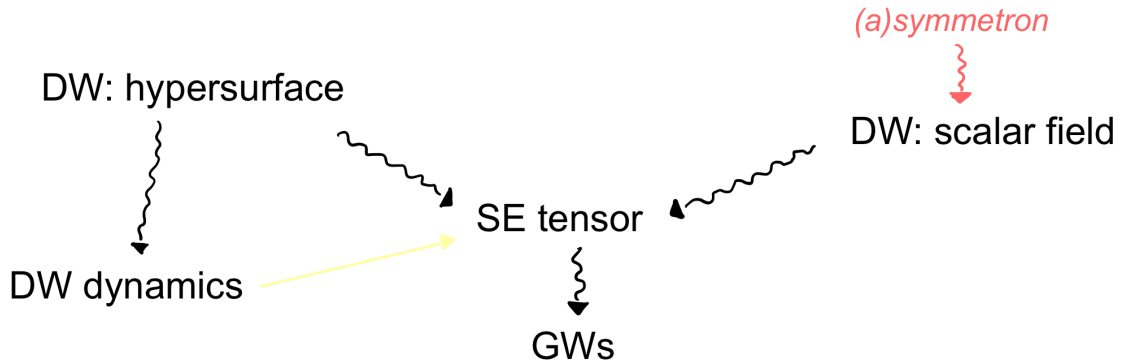
DW: hypersurface

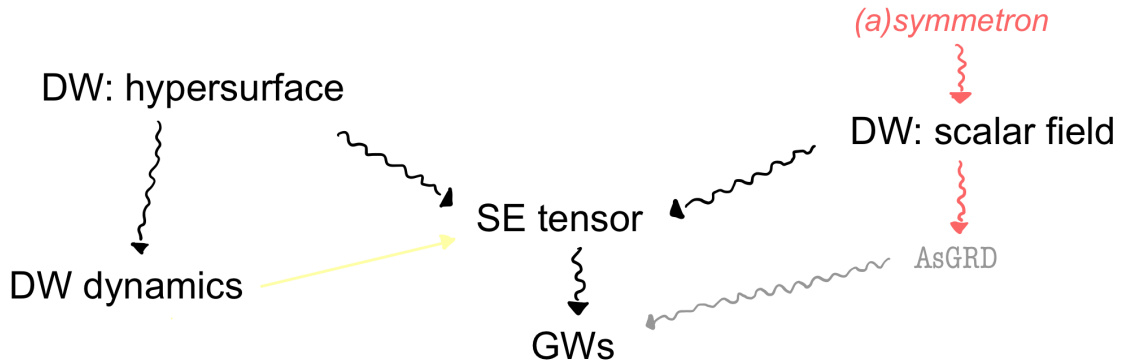
DW: scalar field

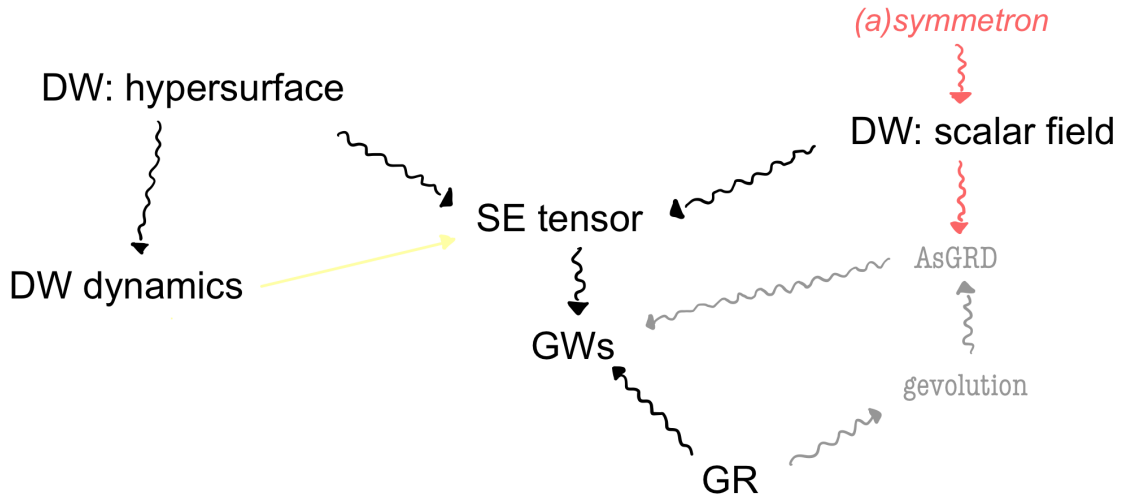


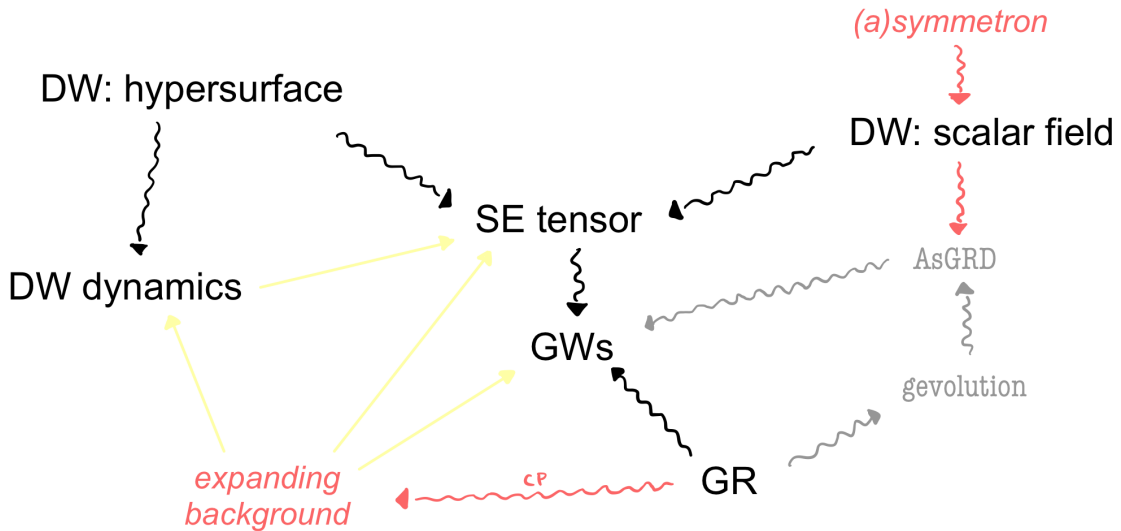
DW: hypersurface

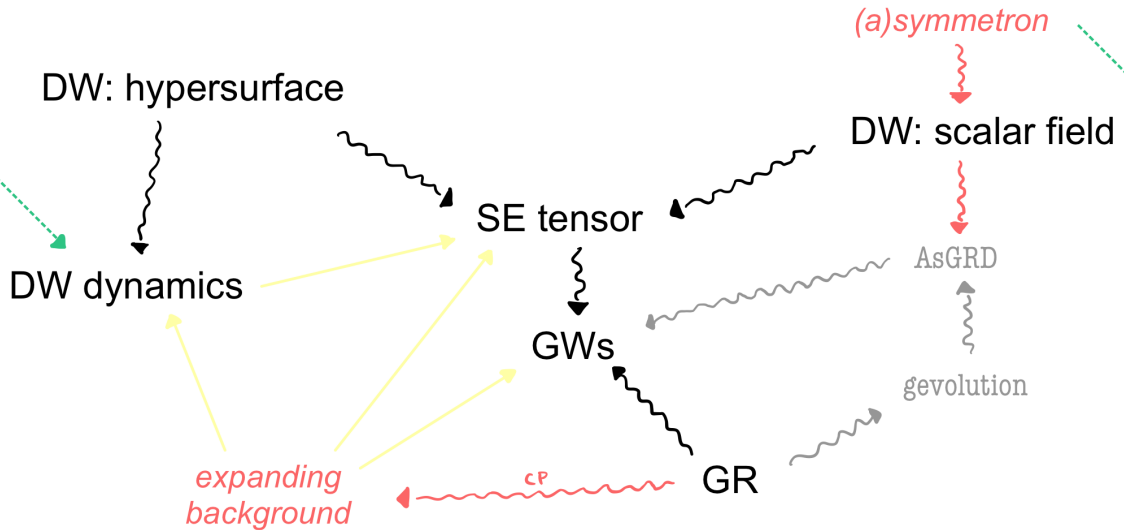












Toy scenario

The (3+1)-dimensional spacetime \mathcal{M} is described by the metric $g_{\mu\nu} = a^2 \eta_{\mu\nu}$ and **Cartesian comoving coordinates** x^μ . We consider a **matter-dominated** ($a \sim \tau^\alpha$, $\alpha = 2$) universe in which a **symmetron** phase transition takes place at scale factor $a = a_*$. This induces the formation of a **domain wall** with (unperturbed) planar structure, oriented perpendicular to the z-axis.

Toy scenario

The (3+1)-dimensional spacetime \mathcal{M} is described by the metric $g_{\mu\nu} = a^2 \eta_{\mu\nu}$ and **Cartesian comoving coordinates** x^μ . We consider a **matter-dominated** ($a \sim \tau^\alpha$, $\alpha = 2$) universe in which a **symmetron** phase transition takes place at scale factor $a = a_*$. This induces the formation of a **domain wall** with (unperturbed) planar structure, oriented perpendicular to the z -axis.

The defect is represented by the hypersurface Σ that splits the ambient spacetime into vacuum domains \mathcal{M}_\pm with energies $v_\pm = v_+$. We let γ_{ab} be the induced metric on the submanifold and impose the coordinate system ξ^a , where $a = 0, 1, 2$. When $n^\mu = \delta^\mu_z$, the hypersurface's energy density—the **surface tension**—is

$$\sigma = - \int_{\Sigma} dz \sqrt{g_{zz}} T^0_0. \quad (6)$$

Alternative toy scenario

The $(N+1)$ -dimensional spacetime \mathcal{M} is described by the metric $g_{\mu\nu} = a^2 \eta_{\mu\nu}$ and arbitrary coordinates x^μ . We consider a [perfect fluid]-dominated ($a \sim \tau^\alpha$, $\alpha \in \mathbb{R}$) universe in which a first-order phase transition takes place at scale factor $a = a_*$. This induces the formation of a topological defect with (unperturbed) simple structure, oriented perpendicular to the unit-normal n^μ .

The defect is represented by the hypersurface Σ that splits the ambient spacetime into vacuum domains \mathcal{M}_\pm with energies v_\pm . We let γ_{ab} be the induced metric on the submanifold and impose the coordinate system ξ^a , where $a = 0, 1, \dots, N - 1$. When $n^\mu = \delta_z^\mu$, the hypersurface's energy density is

$$\mathcal{E} = - \int_{\Sigma} dz \sqrt{g_{zz}} T^0_0. \quad (6)$$

DW ↔ hypersurface

First approach

DW \leftrightarrow hypersurface

Wall positioned at $X^\mu = \delta^\mu_a \xi^a + \delta^\mu_z (z_0 + \epsilon) = (\tau, x, y, z_0 + \epsilon)$.

The induced metric is

$$\gamma_{ab} \equiv a^2 \hat{\gamma}_{ab} = a^2 \eta_{\mu\nu} \partial_a X^\mu \partial_b X^\nu$$

and $\epsilon(\xi^a)$ is a first-order displacement to the wall's z-coordinate.

We have $a = a_* (\tau/\tau_*)^\alpha = a_* (\tau/\tau_*)^2$ and let a dot signify conformal time derivative;
 $\dot{f} \equiv df/d\tau$.

DW \leftrightarrow hypersurface

Wall positioned at $X^\mu = \delta^\mu_a \xi^a + \delta^\mu_z (z_0 + \epsilon) = (\tau, x, y, z_0 + \epsilon)$.

The Nambu-Goto action

$$S_{\text{NG}} = -\sigma \int_{\Sigma} d^3\xi \sqrt{-\gamma} = -\sigma \int_{\Sigma} d^3\xi \sqrt{-\hat{\gamma}} a^3 \quad (7)$$

gives the equation of motion (e.o.m.)

$$\ddot{\epsilon} + \mathcal{D}(\tau) \dot{\epsilon} - [\partial_x^2 + \partial_y^2] \epsilon = 0 \quad (8)$$

where $\mathcal{D}(\tau) = 3\dot{a}/a$.

DW \leftrightarrow hypersurface

Wall positioned at $X^\mu = \delta^\mu_a \xi^a + \delta^\mu_z (z_0 + \epsilon) = (\tau, x, y, z_0 + \epsilon)$.

The **Nambu-Goto action** with time-dependent surface tension

$$S_{\text{NG}} = - \int_{\Sigma} d^3\xi \sqrt{-\gamma} \sigma = - \int_{\Sigma} d^3\xi \sqrt{-\hat{\gamma}} a^3 \sigma \quad (7)$$

gives the equation of motion (e.o.m.)

$$\ddot{\epsilon} + \mathcal{D}(\tau) \dot{\epsilon} - [\partial_x^2 + \partial_y^2] \epsilon = 0 \quad (8)$$

where $\mathcal{D}(\tau) = 3\dot{a}/a + \dot{\sigma}/\sigma$.

Domain-wall dynamics

Separable equation \leadsto Solutions $\epsilon(\tau, x, y) \sim \sum_p \varepsilon(\tau) \cdot \mathcal{E}(x, y)$, where

$$\ddot{\varepsilon} + \mathcal{D}\dot{\varepsilon} = -p^2\varepsilon, \quad (9a)$$

$$[\partial_x^2 + \partial_y^2]\mathcal{E} = -p^2\mathcal{E}, \quad (9b)$$

are the solutions with eigenvalue $-p^2$.

Domain-wall dynamics

Separable equation \leadsto Solutions $\epsilon(\tau, x, y) \sim \sum_p \epsilon(\tau) \cdot \mathcal{E}(x, y)$, where

$$\ddot{\epsilon} + \mathcal{D}\dot{\epsilon} = -p^2\epsilon, \quad (9a)$$

$$[\partial_x^2 + \partial_y^2]\mathcal{E} = -p^2\mathcal{E}, \quad (9b)$$

are the solutions with eigenvalue $-p^2$.

Introduce $s \equiv \tau/\tau_*$ and $\omega \equiv p\tau_*$ such that ($\sigma' = 0$)

$$\epsilon'' + (6/s)\epsilon' + \omega^2\epsilon = 0. \quad (10)$$

General solution: $\epsilon(s) = s^\nu Z_\nu(\omega s)$; $\nu = (1 - 3\alpha)/2 = -5/2$.

Domain-wall dynamics

Separable equation \leadsto Solutions $\varepsilon(\tau, x, y) \sim \sum_p \varepsilon(\tau) \cdot \mathcal{E}(x, y)$, where

$$\ddot{\varepsilon} + \mathcal{D}\dot{\varepsilon} = -p^2\varepsilon, \quad (9a)$$

$$[\partial_x^2 + \partial_y^2]\mathcal{E} = -p^2\mathcal{E}, \quad (9b)$$

are the solutions with eigenvalue $-p^2$.

Introduce $s \equiv \tau/\tau_*$ and $\omega \equiv p\tau_*$ such that ($\sigma' \neq 0$)

$$\varepsilon'' + (\tau_* \mathcal{D})\varepsilon' + \omega^2\varepsilon = 0. \quad (10)$$

General solution: $\varepsilon(s) = ?$.

Symmetron solution

Symmetron domain walls have $\sigma = \sigma_\infty \sqrt{1 - v}^3$ where $v \equiv (a_*/a)^3 = s^{-6}$, and this gives

$$\varepsilon'' + \left(\frac{6}{s} + 2d(s) \right) \varepsilon' + \omega^2 \varepsilon = 0; \quad d(s) \triangleq \frac{9}{2s(s^6 - 1)}. \quad (11)$$

Initial conditions (ICs): $\varepsilon(s = 1) = \varepsilon_*$ and $\varepsilon'(s = 1) = 0$.

Symmetron solution

Symmetron domain walls have $\sigma = \sigma_\infty \sqrt{1 - v^3}$ where $v \equiv (a_*/a)^3 = s^{-6}$, and this gives

$$\varepsilon'' + \left(\frac{6}{s} + 2d(s) \right) \varepsilon' + \omega^2 \varepsilon = 0; \quad d(s) \triangleq \frac{9}{2s(s^6 - 1)}. \quad (11)$$

Initial conditions (ICs): $\varepsilon(s = 1) = \varepsilon_*$ and $\varepsilon'(s = 1) = 0$. Solve in two regimes and sow together at $s = s_{\text{sow}}$, such that

$$\varepsilon(s) = \begin{cases} \varepsilon^{(\text{I})}(s) & \text{if } s \leq s_{\text{sow}}, \\ \varepsilon^{(\text{II})}(s) & \text{if } s \geq s_{\text{sow}}. \end{cases} \quad (12)$$

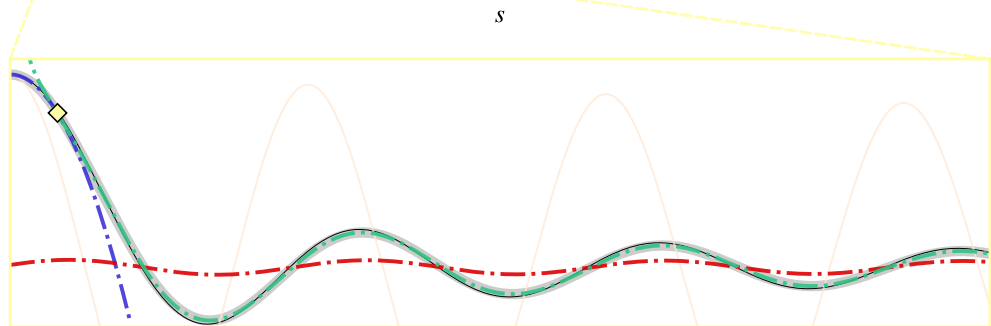
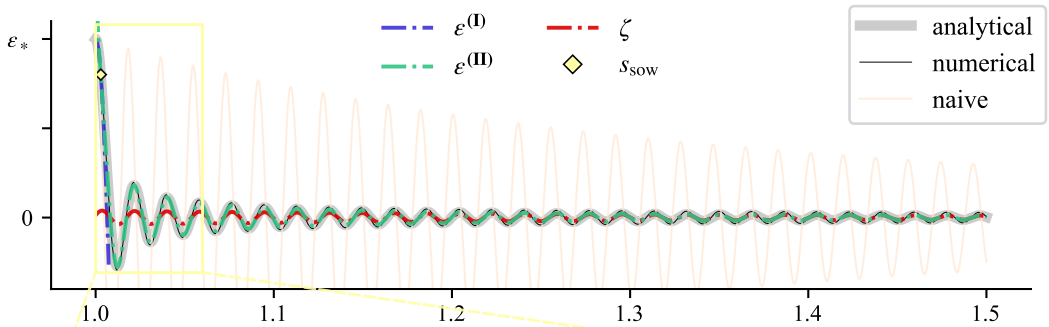
Symmetron solution

Symmetron domain walls have $\sigma = \sigma_\infty \sqrt{1 - v^3}$ where $v \equiv (a_*/a)^3 = s^{-6}$, and this gives

$$\varepsilon'' + \left(\frac{6}{s} + 2d(s) \right) \varepsilon' + \omega^2 \varepsilon = 0; \quad d(s) \triangleq \frac{9}{2s(s^6 - 1)}. \quad (11)$$

Initial conditions (ICs): $\varepsilon(s = 1) = \varepsilon_*$ and $\varepsilon'(s = 1) = 0$. Solve in two regimes and sow together at $s = s_{\text{sow}}$, such that $\varepsilon = \Theta(s_{\text{sow}} - s)\varepsilon^{(\text{I})} + \Theta(s - s_{\text{sow}})\varepsilon^{(\text{II})}$;

$$\begin{aligned} \varepsilon^{(\text{I})}/\varepsilon_* &\simeq 1 - \omega^2(s - 1)^2/5 + \omega^2(s - 1)^3/35, \\ \varepsilon^{(\text{II})}/\varepsilon_* &\simeq \underbrace{\zeta(s) \times s^{9/2}(s^6 - 1)^{-3/4}}_{\text{"naive"}}, \quad \zeta(s) \simeq \underbrace{s^\nu Z_\nu(\omega s)}_{\text{"naive"}}, \nu = -5/2. \end{aligned} \quad (12)$$



Gravitational waves

$$\delta S_{\text{NG}}/\delta g_{\mu\nu} \longrightarrow T^{\mu\nu} \longrightarrow \tilde{T}^{\mu\nu} \longrightarrow \tilde{\pi}_{ij} \longrightarrow \tilde{\pi}_P \longrightarrow \tilde{h}_P$$

The e.o.m. for GWs, $\square h_P = -16\pi G_N \pi_P$, is solved in Fourier space through Green's functions:

$$a\tilde{h}_P(\tau, \mathbf{k}) \propto k^{-2} \int_{\tau_*}^{\tau} d\hat{\tau} G(k\tau, k\hat{\tau}) a^3(\hat{\tau}) \tilde{\pi}_P(\hat{\tau}, \mathbf{k}); \quad P = +, \times, \quad (13)$$

where $G(u, v) = S_1(u)C_1(v) - C_1(u)S_1(v)$.[¶]

We use ICs $\tilde{h}(\tau_*, \mathbf{k}) = \dot{\tilde{h}}(\tau_*, \mathbf{k}) = 0$.

[¶] Riccati-Bessel functions: $S_n(x) = +x j_n(x)$, $C_n(x) = -x y_n(x)$

With $\epsilon = \varepsilon(\tau) \sin(py)$, only *monochromatic plus-polarised GWs* are produced.

For $\ell \equiv k_y/p \in \mathbb{Z}$ and $\vartheta \equiv \arctan(k_y/k_z) \in [0, 2\pi)$, we have

$$a\tilde{\pi}_+ \propto \sigma \cos^2 \vartheta \cdot J_{-\ell}(\ell \tan \vartheta \cdot p\varepsilon). \quad (14)$$

Finally,

$$a\tilde{h}_+ \propto \int_{\tau_*}^{\tau} d\hat{\tau} G(k\tau, k\hat{\tau}) \hat{\tau}^4 \sqrt{1 - (\tau_*/\hat{\tau})^6} J_\ell(\ell \tan \vartheta \cdot p\varepsilon(\hat{\tau})). \quad (15)$$

With $\epsilon = \epsilon(\tau) \sin(py)$, only *monochromatic plus-polarised GWs* are produced.

For $\ell \equiv k_y/p \in \mathbb{Z}$ and $\vartheta \equiv \arctan(k_y/k_z) \in [0, 2\pi)$, we have

$$a\tilde{\pi}_+ \propto \sigma \cos^2 \vartheta \cdot J_{-\ell}(\ell \tan \vartheta \cdot p\epsilon). \quad (14)$$

Finally,

$$a\tilde{h}_+ \propto \int_{\tau_*}^{\tau} d\hat{\tau} G(k\tau, k\hat{\tau}) \hat{\tau}^4 \sqrt{1 - (\tau_*/\hat{\tau})^6} J_\ell(\ell \tan \vartheta \cdot p\epsilon(\hat{\tau})). \quad (15)$$

$$\sim \ll Z_{3/2}(k\tau) \times \int d\hat{\tau} Z_{3/2}(k\hat{\tau}) \times J_\ell[Z_{-5/2}(p\hat{\tau})] \times f(\hat{\tau}) \gg$$

With $\epsilon = \epsilon(\tau) \sin(py)$, only *monochromatic plus-polarised GWs* are produced.

For $\ell \equiv k_y/p \in \mathbb{Z}$ and $\vartheta \equiv \arctan(k_y/k_z) \in [0, 2\pi)$, we have

$$a\tilde{\pi}_+ \propto \sigma \cos^2 \vartheta \cdot J_{-\ell}(\ell \tan \vartheta \cdot p\epsilon). \quad (14)$$

Finally,

$$a\tilde{h}_+^{NG,\phi} \propto \int_{\tau_*}^{\tau} d\hat{\tau} G(k\tau, k\hat{\tau}) \hat{\tau}^4 \sqrt{1 - (\tau_*/\hat{\tau})^6}^3 J_\ell(\ell \tan \vartheta \cdot p\epsilon^{NG,\phi}(\hat{\tau})). \quad (15)$$

DW \leftrightarrow scalar field

Second approach

DW \leftrightarrow scalar field

The e.o.m. for the symmetron field $\phi = \phi_\infty \chi$ is $\square \phi = \partial_\phi V_{\text{eff}}$, or

$$\ddot{\chi} + 2(\dot{a}/a)\dot{\chi} - \nabla^2 \chi = -\mu^2 \cdot a^2 [\chi^2 - \chi_+^2] \chi, \quad (16)$$

where $\chi_\pm = \pm \sqrt{1 - v}$; $v = (a_*/a)^3 = s^{-6}$.

DW \leftrightarrow scalar field

The e.o.m. for the symmetron field $\phi = \phi_\infty \chi$ is $\square \phi = \partial_\phi V_{\text{eff}}$, or

$$\ddot{\chi} + 2(\dot{a}/a)\dot{\chi} - \nabla^2 \chi = -\mu^2 \cdot a^2 [\chi^2 - \chi_+^2] \chi, \quad (16)$$

where $\chi_\pm = \pm \sqrt{1 - v}$; $v = (a_*/a)^3 = s^{-6}$.

MINKOWSKI, STATIC CASE. $\chi = \tanh(\mu z/\sqrt{2})$ if $a = 1$ and $\chi_+ = 1$ ($a \gg a_*$)

Quasi-static limit

In the quasi-static limit,^{††}

$$\nabla^2 \chi \simeq \partial_z^2 \chi \simeq \mu^2 \cdot a^2 [\chi^2 - \chi_+^2] \chi, \quad (17)$$

where $\chi_{\pm} = \pm \sqrt{1 - v}$. With boundary conditions (BCs) $\chi|_{z \rightarrow \pm\infty} = \chi_{\pm}$, an approximate solution is

$$\chi_w = \chi_+ \tanh \left(\frac{\chi_+ a(z - z_w)}{2L_c} \right), \quad (18)$$

if we can assume that the derivatives of $z_w = z_0 + \epsilon(\tau, y)$ makes no significant difference.

^{††} $\dot{\chi} \ll \nabla^2 \chi$

Comoving wall thickness

$$\delta_w = \frac{\delta_\infty}{a\sqrt{1-v}} \rightarrow \begin{cases} \infty & \text{for } a \rightarrow a_*, \\ \delta_\infty & \text{for } a \gg a_*, \end{cases} \quad (19)$$

and surface tension

$$\sigma_w = \sigma_\infty [1-v]^{3/2} \rightarrow \begin{cases} 0 & \text{for } a \rightarrow a_*, \\ \sigma_\infty & \text{for } a \gg a_*, \end{cases} \quad (20)$$

where $\delta_\infty = 1/\mu$ and $\sigma_\infty = 2\sqrt{2}\mu^3/(3\lambda)$.

Asymptotic limit

Far away from the wall,^{‡‡} the field takes values $\pm\check{\chi}$, obeying

$$\ddot{\check{\chi}} + 2(\dot{a}/a)\dot{\check{\chi}} = -\mu^2 \cdot a^2 [\check{\chi}^2 - \chi_+^2] \check{\chi}. \quad (21)$$

Generally, $\pm\check{\chi} \sim \chi_{\pm}$, depending on ICs.

^{‡‡} $\nabla^2 \chi \rightarrow 0$

Asymptotic limit

Far away from the wall,^{‡‡} the field takes values $\pm\check{\chi}$, obeying

$$\ddot{\check{\chi}} + 2(\dot{a}/a)\dot{\check{\chi}} = -\mu^2 \cdot a^2 [\check{\chi}^2 - \chi_+^2] \check{\chi}. \quad (21)$$

Generally, $\pm\check{\chi} \sim \chi_{\pm}$, depending on ICs.

STABLE FIELD. We present a protocol for finding the solution with the smallest possible oscillations around χ_+ in Appendix B. This also allows initialisation at PT.

The **farfalle** is the “optimal” solution (Appendix B), **spaghetti** shows the solution with our default ICs, **gnocchi** shows an «unfortunate» solution and the **ravioli** tracks the potential’s positive minimum, $\chi_+ = \sqrt{1 - v}$.

Part II of the animation is zoomed from the **ravioli**’s point of view.

Analysis

Contents

1 Background

2 Project

3 Analysis

- Simulations
- DW
- GWs
- Summary

4 Foreground

The code

AsGRD,^{*} based on `gevolution`,[†] computes the full metric perturbations and is compatible with asymmetron scenarios.

^{*}Christiansen et al. ((2024))

[†]Adamek et al. ((2016))

The code

AsGRD, based on `gevolution`, computes the full metric perturbations and is compatible with asymmetron scenarios.

Cubic simulation boxes with **periodic boundaries** demand the presence of two or more walls.

Experiments

Cubic simulation box of side lengths $L_{\#}$ (fundamental frequency $k_{\#} = 2\pi/L_{\#}$) with $N_{\#}^3$ lattice points, with perturbation $\epsilon_* = \varepsilon_* \sin(py)$ to the middle wall. Fiducial symmetron parameters are $a_* = 0.33$, $\xi_* = 3.33 \times 10^{-4}$ and $\beta_* = 1$ (Thesis, Eq. (5.22)). Complete matter domination ($\Omega_{m0} = 1$) gives $\tau_* \approx 3.4$ Gpc/h. Simulation onset is at scale factor $a_i \gtrsim a_*$, and we finish at $a_f = 0.50$.

Experiments

Cubic simulation box of side lengths $L_{\#}$ (fundamental frequency $k_{\#} = 2\pi/L_{\#}$) with $N_{\#}^3$ lattice points, with perturbation $\epsilon_* = \epsilon_* \sin(py)$ to the middle wall. Fiducial symmetron parameters are $a_* = 0.33$, $\xi_* = 3.33 \times 10^{-4}$ and $\beta_* = 1$ (Thesis, Eq. (5.22)). Complete matter domination ($\Omega_{m0} = 1$) gives $\tau_* \approx 3.4$ Gpc/h. Simulation onset is at scale factor $a_i \gtrsim a_*$, and we finish at $a_f = 0.50$.

1 $\epsilon_* = 0.08L_{\#}, p = 2k_{\#}, L_{\#} \approx 1$ Gpc/h, $N_{\#} = 768, a_i \simeq a_* + 0.003$

Experiments

Cubic simulation box of side lengths $L_{\#}$ (fundamental frequency $k_{\#} = 2\pi/L_{\#}$) with $N_{\#}^3$ lattice points, with perturbation $\epsilon_* = \epsilon_* \sin(py)$ to the middle wall. Fiducial symmetron parameters are $a_* = 0.33$, $\xi_* = 3.33 \times 10^{-4}$ and $\beta_* = 1$ (Thesis, Eq. (5.22)). Complete matter domination ($\Omega_{m0} = 1$) gives $\tau_* \approx 3.4$ Gpc/h. Simulation onset is at scale factor $a_i \gtrsim a_*$, and we finish at $a_f = 0.50$.

$$1 \quad \epsilon_* = 0.08L_{\#}, p = 2k_{\#}, L_{\#} \approx 1 \text{ Gpc/h}, N_{\#} = 768, a_i \simeq a_* + 0.003$$

$$2 \quad \epsilon_* \rightarrow 0.12L_{\#}$$

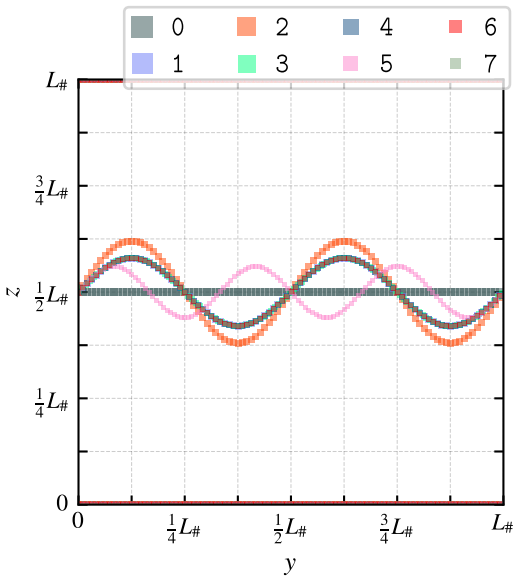
$$3 \quad N_{\#} \rightarrow 900$$

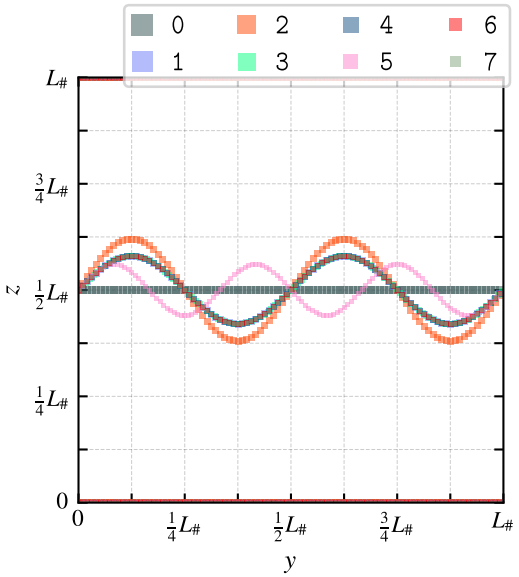
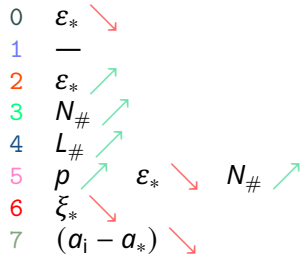
$$4 \quad L_{\#} \rightarrow 1.4 \text{ Gpc/h}$$

$$5 \quad p \rightarrow 3k_{\#}, \epsilon_* \rightarrow 0.06L_{\#}, N_{\#} \rightarrow 900$$

$$7 \quad (a_i - a_*) \rightarrow 0.001$$

1 —
 2 ε_*
 3 $N_\#$
 4 $L_\#$
 5 p ε_* $N_\#$
 7 $(a_i - a_*)$





Wall displacement field

Center wall's z-position $z_w = z_0 + \epsilon(\tau, x, y)$ where $z_0 = \mathfrak{D} \equiv L_{\#}/2$ is the unperturbed position and $\epsilon(\tau, x, y) = \varepsilon(\tau) \sin(py)$ the displacement field.

Wall displacement field

Center wall's z-position $z_w = z_0 + \epsilon(\tau, x, y)$ where $z_0 = \mathfrak{D} \equiv L_{\#}/2$ is the unperturbed position and $\epsilon(\tau, x, y) = \varepsilon(\tau) \sin(py)$ the displacement field.

FIRST APPROACH $\sim \varepsilon(\tau) = \varepsilon^{\text{NG}}(\tau)$, analytically determined in the thin-wall limit

Wall displacement field

Center wall's z-position $z_w = z_0 + \epsilon(\tau, x, y)$ where $z_0 = \mathfrak{D} \equiv L_{\#}/2$ is the unperturbed position and $\epsilon(\tau, x, y) = \varepsilon(\tau) \sin(py)$ the displacement field.

FIRST APPROACH $\sim \varepsilon(\tau) = \varepsilon^{\text{NG}}(\tau)$, analytically determined in the thin-wall limit

SECOND APPROACH $\sim \varepsilon(\tau) = \varepsilon^\phi(\tau)$, from the coordinate at which the simulated field $|\chi|$ takes its minimum value along a slice at a y-coordinate that satisfies $\sin(py) = 1$

Wall displacement field

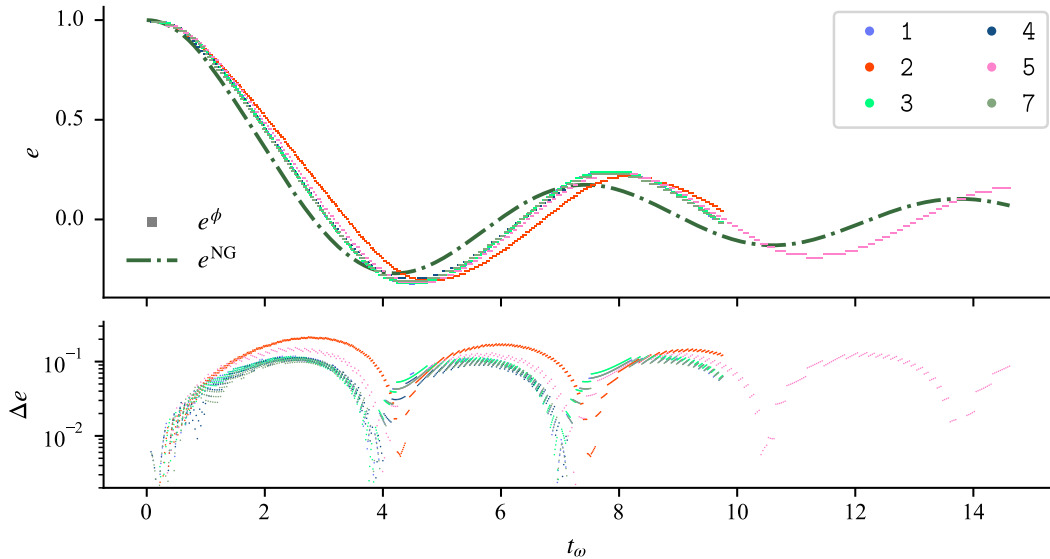
Center wall's z-position $z_w = z_0 + \epsilon(\tau, x, y)$ where $z_0 = \mathfrak{D} \equiv L_{\#}/2$ is the unperturbed position and $\epsilon(\tau, x, y) = \varepsilon(\tau) \sin(py)$ the displacement field.

FIRST APPROACH $\sim \varepsilon(\tau) = \varepsilon^{\text{NG}}(\tau)$, analytically determined in the thin-wall limit

SECOND APPROACH $\sim \varepsilon(\tau) = \varepsilon^\phi(\tau)$, from the coordinate at which the simulated field $|\chi|$ takes its minimum value along a slice at a y-coordinate that satisfies $\sin(py) = 1$

We do **not** expect a perfect match.

Wall position $e = \varepsilon/\varepsilon_*$ as functions of $t_\omega = p(\tau - \tau_*)$



$$e \equiv \varepsilon/\varepsilon_*, \quad \Delta e \equiv |e^{\text{NG}} - e^\phi|, \quad t_\omega = \omega(s-1)$$

Gravitational waves

We have GWs in Fourier space with $\mathbf{k} = (k_x, k_y, k_z) = (u, v, w)k_\#.$

Gravitational waves

$$a\tilde{h}_+^{\text{NG},\phi} \propto \int d\hat{\tau} [\dots] \times J_\ell([\dots]\rho\varepsilon^{\text{NG},\phi})$$

We have GWs in Fourier space with $\mathbf{k} = (k_x, k_y, k_z) = (\mathbf{u}, \mathbf{v}, \mathbf{w})k_\#$.

\tilde{h}_+^{NG} \leftrightarrow semi-analytical formula with ε^{NG} as input to the SE tensor

\tilde{h}_+^ϕ \leftrightarrow semi-analytical formula with ε^ϕ as input to the SE tensor

Gravitational waves

$$a\tilde{h}_+^{\text{NG},\phi} \propto \int d\hat{\tau} [\dots] \times J_\ell([\dots]\rho\varepsilon^{\text{NG},\phi})$$

We have GWs in Fourier space with $\mathbf{k} = (k_x, k_y, k_z) = (\mathbf{u}, \mathbf{v}, \mathbf{w})k_\#$.

\tilde{h}_+^{NG} \leftrightarrow semi-analytical formula with ε^{NG} as input to the SE tensor

\tilde{h}_+^ϕ \leftrightarrow semi-analytical formula with ε^ϕ as input to the SE tensor

\tilde{h}_+ \leftrightarrow output from AsGRD

Gravitational waves

$$a\tilde{h}_+^{\text{NG},\phi} \propto \int d\hat{\tau} [\dots] \times J_\ell([\dots] p \varepsilon^{\text{NG},\phi})$$

We have GWs in Fourier space with $\mathbf{k} = (k_x, k_y, k_z) = (\mathbf{u}, \mathbf{v}, \mathbf{w})k_\#$.

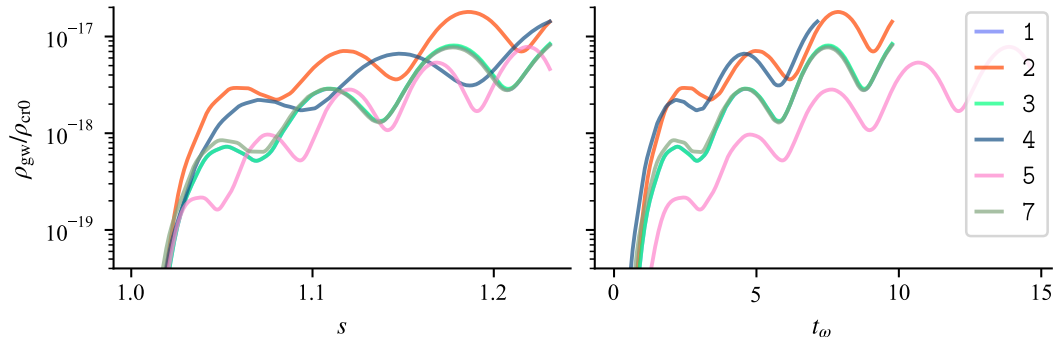
\tilde{h}_+^{NG} \leftrightarrow semi-analytical formula with ε^{NG} as input to the SE tensor

\tilde{h}_+^ϕ \leftrightarrow semi-analytical formula with ε^ϕ as input to the SE tensor

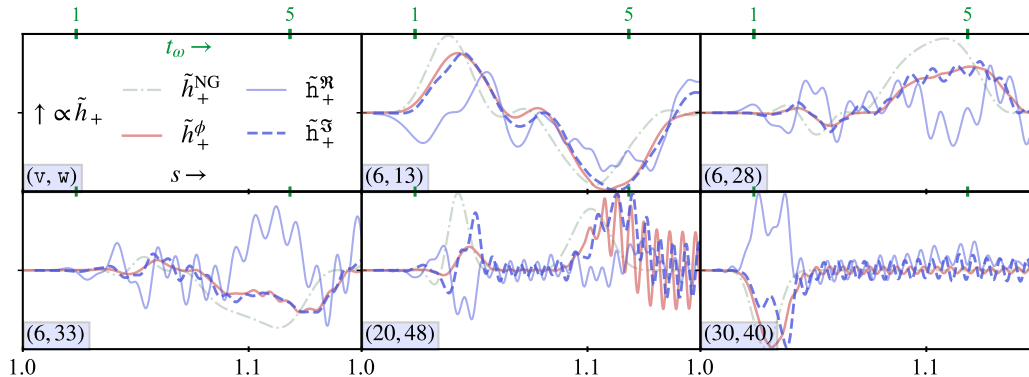
\tilde{h}_+ \leftrightarrow output from AsGRD

MAGNITUDES. The magnitudes differ unsystematically in between these three, and we will not address this issue here.

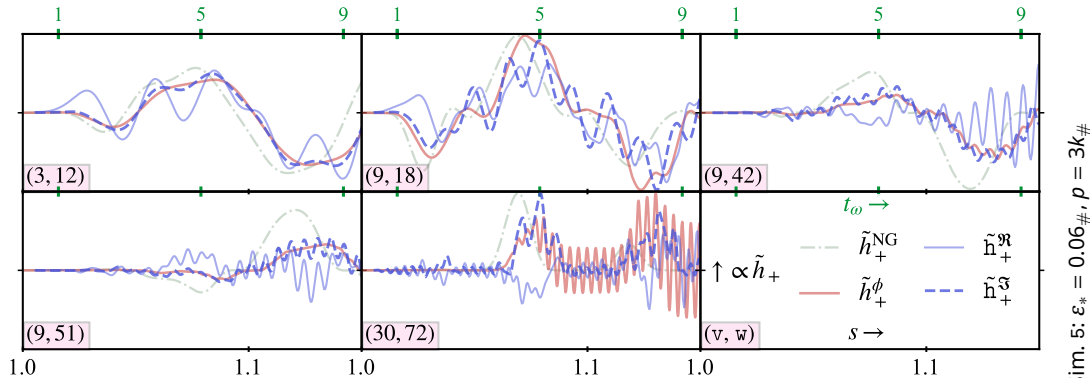
$$\text{Gravitational radiation } \rho_{\text{gw}} = M_{\text{Pl}}^2 a^{-2} \langle \dot{h}^{ij} \dot{h}_{ij} \rangle$$



$$s = \tau / \tau_* , \quad t_\omega = \omega(s - 1)$$



Sim. 1: $\varepsilon_* = 0.08\#$, $\rho = 2k\#$



	Calculation	Simulation
<i>Wall position, $e = \varepsilon/\varepsilon_*$</i>	e^{NG}	e^ϕ
<i>Gravitational waves</i>	$\tilde{h}_+^{\text{NG},\phi}$	\tilde{h}_+

	Calculation	Simulation
<i>Wall position, $e = \varepsilon/\varepsilon_*$</i>	e^{NG}	e^ϕ
e independent of ε_*	yes	no
<i>Gravitational waves</i>	$\tilde{h}_+^{\text{NG},\phi}$	\tilde{h}_+

	Calculation	Simulation
<i>Wall position, $e = \varepsilon/\varepsilon_*$</i>	e^{NG}	e^ϕ
e independent of ε_*	yes	no
$e \sim s^{-5/2} Z_{-5/2}(\omega s)$	no	no
<i>Gravitational waves</i>	$\tilde{h}_+^{\text{NG},\phi}$	\tilde{h}_+

* To some extent.

	Calculation	Simulation
<i>Wall position, $e = \varepsilon/\varepsilon_*$</i>	e^{NG}	e^ϕ
e independent of ε_*	yes	no
$e \sim s^{-5/2} Z_{-5/2}(\omega s)$	no	no
(e vs. t_ω)-plot indep. of parameters	yes	yes*
<i>Gravitational waves</i>	$\tilde{h}_+^{\text{NG},\phi}$	\tilde{h}_+

* To some extent.

	Calculation	Simulation
<i>Wall position, $e = \varepsilon/\varepsilon_*$</i>	e^{NG}	e^ϕ
e independent of ε_*	yes	no
$e \sim s^{-5/2} Z_{-5/2}(\omega s)$	no	no
(e vs. t_ω)-plot indep. of parameters	yes	yes*
e unaffected by large fifth-force oscillations	yes*	yes*
<i>Gravitational waves</i>	$\tilde{h}_+^{\text{NG},\phi}$	\tilde{h}_+

* To some extent.

	Calculation	Simulation
<i>Wall position, $e = \varepsilon/\varepsilon_*$</i>	e^{NG}	e^ϕ
e independent of ε_*	yes	no
$e \sim s^{-5/2} Z_{-5/2}(\omega s)$	no	no
(e vs. t_ω)-plot indep. of parameters	yes	yes*
e unaffected by large fifth-force oscillations	yes*	yes*
<i>Gravitational waves</i>	$\tilde{h}_+^{\text{NG},\phi}$	\tilde{h}_+
$\tilde{h}_x = 0$	yes	yes

* To some extent.

	Calculation	Simulation
<i>Wall position, $e = \varepsilon/\varepsilon_*$</i>	e^{NG}	e^ϕ
e independent of ε_*	yes	no
$e \sim s^{-5/2} Z_{-5/2}(\omega s)$	no	no
(e vs. t_ω)-plot indep. of parameters	yes	yes*
e unaffected by large fifth-force oscillations	yes*	yes*
<i>Gravitational waves</i>	$\tilde{h}_+^{\text{NG},\phi}$	\tilde{h}_+
$\tilde{h}_x = 0$	yes	yes
$\tilde{h}_+ \in \mathbb{R}$	yes	no

* To some extent.

	Calculation	Simulation
<i>Wall position, $e = \varepsilon/\varepsilon_*$</i>	e^{NG}	e^ϕ
e independent of ε_*	yes	no
$e \sim s^{-5/2} Z_{-5/2}(\omega s)$	no	no
(e vs. t_ω)-plot indep. of parameters	yes	yes*
e unaffected by large fifth-force oscillations	yes*	yes*
<i>Gravitational waves</i>	$\tilde{h}_+^{\text{NG},\phi}$	\tilde{h}_+
$\tilde{h}_x = 0$	yes	yes
$\tilde{h}_+ \in \mathbb{R}$	yes	no
$\tilde{h}_+ \simeq 0$ for $k_x \neq 0$, and for $k_y \neq np$	yes	yes

* To some extent.

	Calculation	Simulation
<i>Wall position, $e = \varepsilon/\varepsilon_*$</i>	e^{NG}	e^ϕ
e independent of ε_*	yes	no
$e \sim s^{-5/2} Z_{-5/2}(\omega s)$	no	no
(e vs. t_ω)-plot indep. of parameters	yes	yes*
e unaffected by large fifth-force oscillations	yes*	yes*
<i>Gravitational waves</i>	$\tilde{h}_+^{\text{NG},\phi}$	\tilde{h}_+
$\tilde{h}_x = 0$	yes	yes
$\tilde{h}_+ \in \mathbb{R}$	yes	no
$\tilde{h}_+ \simeq 0$ for $k_x \neq 0$, and for $k_y \neq np$	yes	yes
$\tilde{h}_+ = 0$ for $k_y = 0$	yes	no

* To some extent.

Foreground

Contents

1 Background

2 Project

3 Analysis

4 Foreground

- Way forward
- Conclusion

Possible ways forward

Testing the limits of the framework ↗
Comparing thin-wall description to full-theory simulations...

Possible ways forward

- Perform higher-resolution experiments.
 - Dissociate discrepancies due to numerical limitations.
 - Investigate the effect of changing the wall thickness.

Possible ways forward

- Perform higher-resolution experiments.
- Investigate the effect of a Yukawa-like force term,

$$\ddot{\epsilon} \supset A \exp(-\mu \mathfrak{d}), \quad \mathfrak{d} \triangleq |\mathfrak{D} - \epsilon(\tau, y)|.$$

Possible ways forward

- Perform higher-resolution experiments.
- Investigate the effect of a Yukawa-like force term, $\ddot{e} \supset A \exp(-\mu d)$.
- Find suitable statistical measures for the GWs.
 - Perhaps asymptotic analyses are the ways to go.

Possible ways forward

- Perform higher-resolution experiments.
- Investigate the effect of a Yukawa-like force term, $\ddot{e} \supset A \exp(-\mu d)$.
- Find suitable statistical measures for the GWs.

*Further development of the framework ↗
Assume limitations are well understood...*

Possible ways forward

- Perform higher-resolution experiments.
- Investigate the effect of a Yukawa-like force term, $\ddot{e} \supset A \exp(-\mu d)$.
- Find suitable statistical measures for the GWs.
- Vary parameters of the theory.
 - Establish relationship between symmetron parameters μ , λ and M , and GW signature.

Possible ways forward

- Perform higher-resolution experiments.
- Investigate the effect of a Yukawa-like force term, $\ddot{\epsilon} \supset A \exp(-\mu d)$.
- Find suitable statistical measures for the GWs.

- Vary parameters of the theory.
- Apply more complicated displacement ϵ .
 - $\epsilon = \epsilon(\tau) \sin(py)$ is the simplest non-trivial solution, and a very unlikely configuration.

Possible ways forward

- Perform higher-resolution experiments.
- Investigate the effect of a Yukawa-like force term, $\ddot{e} \supset A \exp(-\mu d)$.
- Find suitable statistical measures for the GWs.

- Vary parameters of the theory.
- Apply more complicated displacement e .
- Introduce energy bias $v = v_+ - v_- \neq 0$.
 - Does it change the motion significantly?
 - Are there analytical solutions for this?

Possible ways forward

- Perform higher-resolution experiments.
- Investigate the effect of a Yukawa-like force term, $\ddot{e} \supset A \exp(-\mu d)$.
- Find suitable statistical measures for the GWs.
- Vary parameters of the theory.
- Apply more complicated displacement e .
- Introduce energy bias $v = v_+ - v_- \neq 0$.

Concluding remarks

- Analytical solution ϵ^{NG} is not found in other literature (to the best of our knowledge).
- Formula for gravitational waves needs further validation.
- Solid foundation is laid for further similar analyses with AsGRD.

References

- Adamek, J., Daverio, D., Durrer, R., & Kunz, M. 2016, Nature Physics, 12, 346
- Agazie, G., Alam, M. F., Anumarlapudi, A., et al. 2023, The Astrophysical Journal, 951, L9
- Christiansen, Ø., Adamek, J., Hassani, F., & Mota, D. F. 2024, Gravitational Waves from Dark Domain Walls
- Hinterbichler, K., Khouri, J., Levy, A., & Matas, A. 2011, Physical Review D, 84, 103521
- Perivolaropoulos, L. & Skara, F. 2022, Physical Review D, 106, 043528
((All figures are created by the author.))

Nanna Bryne

Spacetime Ripples from Domain-Wall Wiggles

On the analytical prediction of the gravitational-wave signature from perturbed topological defects in expanding spacetime